

# Intercellular Connections Related to Cell–Cell Crosstalk Specifically Recognized by an Aptamer

Nan Zhang, Tao Bing, Luyao Shen, Rusheng Song, Linlin Wang, Xiangjun Liu, Meirong Liu, Juan Li, Weihong Tan,\* and Dihua Shangguan\*

**Abstract:** Intercellular connections are an important pathway for cell–cell crosstalk. However, their formation mechanism and functions are far from being understood. The lack of molecular probes hampers the research in this area. Herein, we report a kind of intercellular connection that is specifically recognized by aptamer M17A2 generated by cell-SELEX against MCF-7R cells. These connections have different morphologies, but have the same skeleton composed of F-actin. The long filamentous connections were identified to be tunneling nanotubes (TNTs), a recently discovered cell–cell communication route. These connections could be built not only between MCF-7R cells, but also from MCF-7R to other cells after co-culture. Proteins could be transported between cells through these connections, suggesting their cell communication function. Aptamer M17A2 shows the potential to act as a new probe for investigating this kind of intercellular connection, as well as for studying cell–cell communication.

Intercellular crosstalk can be defined as the process of exchanging molecular messages and materials between cells, and while it plays an important role in maintaining physiological activities, it is also involved in cancer pathogenesis and invasion.<sup>[1]</sup> In animals, cell–cell crosstalk is mediated through

ligand–receptor signaling pathways or secretion/uptake of exosome-transmitting information across the surrounding intercellular environment.<sup>[2]</sup> Cell–cell crosstalk is also enabled through the use of intercellular structures, such as synapses,<sup>[3]</sup> gap junctions,<sup>[4]</sup> filopodial bridges<sup>[5]</sup> and tunneling nanotubes (TNTs),<sup>[6]</sup> directly trafficking signaling molecules or organelles between connected cells. TNTs were first observed between animal cells in 1999, and later were verified as a novel intercellular communication route, transporting diverse cellular contents, as well as electrical signals.<sup>[6]</sup> They are characterized as membrane channels that consist of filament actin (F-actin), and link two cell cytoplasms over a distance as long as several cell diameters without contacting the substratum.<sup>[7]</sup> Due to the lack of protein markers, morphology and cytoskeletal components are currently the main criteria for classification and identification of intercellular structures, for example, TNTs.<sup>[7b,e,8]</sup> The fundamental mechanisms underlying the formation and functions of most intercellular structures remain unclear. Therefore, probes able to specifically recognize intercellular structures can provide a better understanding of their formation and functions.

Aptamers are single-stranded oligonucleotides with high specificity and affinity to their molecular targets. They are evolved from a random oligonucleotide library by a repetitive target binding process known as Systematic Evolution of Ligands by EXponential enrichment (SELEX).<sup>[9]</sup> Recently, cell-SELEX, a SELEX process that uses whole living cells as targets, has exhibited the ability to generate aptamers able to bind molecular signatures on the target cells.<sup>[10]</sup> Given the advantages of aptamers over antibodies, such as flexible modification, good stability, no immunogenicity, low molecular weight, and easy chemical synthesis,<sup>[11]</sup> aptamers generated by cell-SELEX have shown wide utility in cell capture, detection, and imaging.<sup>[12]</sup> For a specific cell type, such as cancer cells, cell-surface molecular signatures are far from being understood. Therefore, cell-SELEX provides the opportunity to generate aptamers that recognize previously unknown proteins on the cell surface, in turn leading to the discovery of new molecular events. Herein, we present a cell-SELEX-generated aptamer that selectively binds intercellular connections related to cell–cell crosstalk (Figure 1). To our knowledge, this is the first report of its kind.

To investigate the molecular events of cancer cell drug resistance, we performed cell-SELEX using a doxorubicin-resistant breast cancer cell line (MCF-7R) as target cells and its parental cell line (MCF-7) for counter-selection (negative). A detailed description of aptamer selection and generation is given in the Supporting Information and Figure S1. After

[\*] N. Zhang, Prof. T. Bing, L. Shen, R. Song, L. Wang, Prof. X. Liu, M. Liu, Prof. D. Shangguan  
Beijing National Laboratory for Molecular Sciences  
Key Laboratory of Analytical Chemistry for Living Biosystems  
Institute of Chemistry, Chinese Academy of Sciences  
Beijing, 100190 (P.R. China)  
E-mail: sgdh@iccas.ac.cn

N. Zhang, L. Shen, R. Song, L. Wang  
University of the Chinese Academy of Sciences  
Beijing, 100049 (P.R. China)

Dr. J. Li, Prof. W. Tan  
Department of Chemistry  
Center for Research at the Bio/Nano Interface  
Health Cancer Center, UF Genetics Institute  
McKnight Brain Institute, University of Florida  
Gainesville, FL 32611-7200 (USA)  
and

Molecular Science and Biomedicine Laboratory  
State Key Laboratory of Chemo/Bio-Sensing and Chemometrics  
College of Biology and  
College of Chemistry and Chemical Engineering  
Hunan University  
Changsha, 410082 (P.R. China)  
E-mail: tan@chem.ufl.edu

Supporting information and the ORCID identification number(s) for the author(s) of this article can be found under <http://dx.doi.org/10.1002/anie.201510786>.

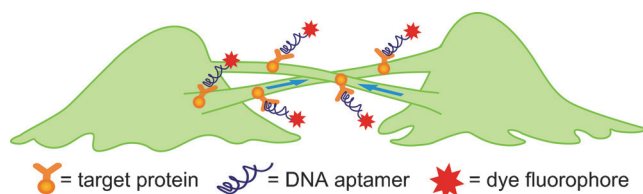


**Figure 1.** Intercellular connections that are specifically recognized by aptameric probe generated by cell-SELEX.

seventeen rounds of selection, four aptamer sequences (Table S1) were found to bind MCF-7R cells, but not MCF-7 and other cell lines, including 18 cancer cell lines and a normal cell line (Figure 2a,b; Supporting Information,

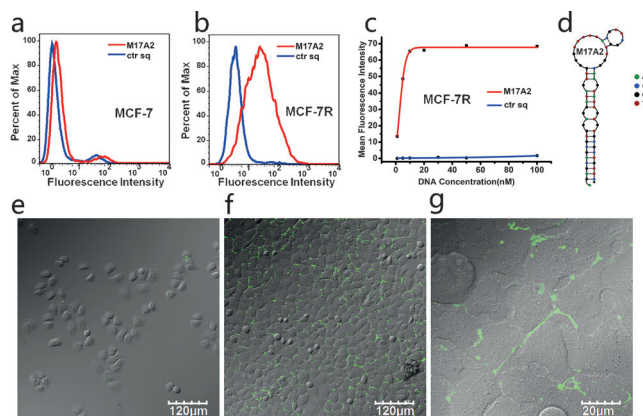


**Figure 2.** Characterization of aptamer M17A2. a, b) Flow cytometry assay of M17A2 binding to negative cell MCF-7 (a) and target cell MCF-7R (b). M17A2 (red lines); ctr sq (blue lines), negative control sequence. c) Binding curve of M17A2 to MCF-7R. d) Secondary structure of M17A2. e, f) Confocal images of M17A2 binding MCF-7R cells at low (e) and high (f) density (20× objective lens). g) M17A2 binding MCF-7R cells at high density (100× oil objective lens).

Figures S2 and S3). Among the recovered sequences, aptamer M17A2 exhibited the strongest binding affinity and could compete with three other aptamers for MCF-7R binding (Figure S4), thus warranting further investigation.

Binding assay showed that M17A2 exhibited high affinity to MCF-7R cells at 4°C and 37°C (Figure 2b and S5). The equilibrium dissociation constant was measured to be  $2.72 \pm 1.05 \text{ nmol L}^{-1}$  at 4°C (Figure 2c). The secondary structure of M17A2, as predicted by Nupack,<sup>[13]</sup> showed a hairpin structure with bulges and attached loop (Figure 2d). Pretreatment of MCF-7R cells with trypsin or proteinase K caused complete loss of their binding ability to M17A2 (Figure S6), suggesting that the target of M17A2 is a membrane protein. In addition, the intact M17A2 was recovered from MCF-7R cells after incubation with M17A2 for 30 or 60 min at 37°C by trypsin treatment (Figure S7), suggesting the integrity of the aptamer binding on cells.

Other aptamers generated by cell-SELEX usually bind to the periphery of cells, such as previously reported aptamer sgc8<sup>[14]</sup> bound to the body of MCF-7R cells (Figure S8). In

contrast, M17A2 was observed to mainly bind structures connecting cells, based on the distance between cells, some reaching up to 50 μm or longer (Figure 2g, S3, and S8). Flow cytometry showed that MCF-7R cells stained by dye-labeled M17A2 have a much broader fluorescence distribution than those stained by dye-labeled sgc8, suggesting that the amount of the molecular target of M17A2 on MCF-7R cells varied greatly (Figure 2b; Supporting Information, Figure S8). Additionally, the fluorescence intensity of M17A2-bound MCF-7R cells was found to be positively correlated with the growth density of cells (Figure 2e,f; Supporting Information, Figure S9,S10). Thus, at low cell density, only a few fluorescent dots were observed on individual cells, while at high cell density, many fluorescent regions were found between cells. These results suggest that M17A2 could be binding connective, or cell-bridging, structures.

To identify the intercellular connections bound by M17A2, we used a plasma membrane probe (Fluorescein-conjugated lectin wheat germ agglutinin (FITC-WGA)) and rhodamine-labeled M17A2 to dual-stain MCF-7R cells (Figure 3a; Supporting Information, Figure S11). Interestingly, M17A2 did not bind with the whole membrane, but rather, the connective regions between two cells, or long filamentous structures between separate cells, or across several cells (Figure S11b). Figure 3b shows a typical ultrafine structure with a diameter less than 500 nm and length up to 40 μm. The three-dimensional reconstructed image (Z-stack image) showed a bridge-like structure extended in intercellular space without contacting the substrate. The morphological features of this filamentous structure imply that it may be a TNT or TNT-like structure. Apart from the morphological features and functional description noted above, the skeleton of TNT was previously found to be polymerized by F-actin, instead of tubulin.<sup>[15]</sup> Accordingly, an F-actin probe (FITC-labeled phalloidin) and a tubulin probe (Tubulin Tracker Red) were, respectively, used to stain MCF-7R cells, together with dye-labeled-M17A2. As shown in Figure 3c and 3d, the aptamer-binding structures were stained by F-actin probe, but not by the tubulin probe, indicating that these structures are composed of F-actin. In addition, cytochalasin B (CB) was reported to selectively block TNT formation by inhibiting the outgrowth of filopodia, the precursor of TNTs.<sup>[16]</sup> To make this determination in the present study, MCF-7R cells were treated with cytochalasin B overnight, and, as expected, M17A2 binding decreased sharply (>60% fluorescence decrease), while sgc8 binding was only slightly affected (<20% fluorescence decrease; Figure 3e), suggesting that the inhibition of TNT formation decreased the binding of M17A2. Taken together, these results suggest that the intercellular connections selectively recognized by M17A2 are homologous with TNTs. TNTs have been reported to be formed by MCF-7 cells.<sup>[1]</sup> We also observed TNT-like structures between MCF-7 cells by staining cells with FITC-WGA, FITC-phalloidin, and Tubulin Tracker Red (Figure S12). However, these structures could not be bound by M17A2, suggesting that structural compositions of TNTs or TNT-like structures may differ between cell lines.

TNTs or TNT-like structures have been reported as a type of intercellular communication route that facilitates the



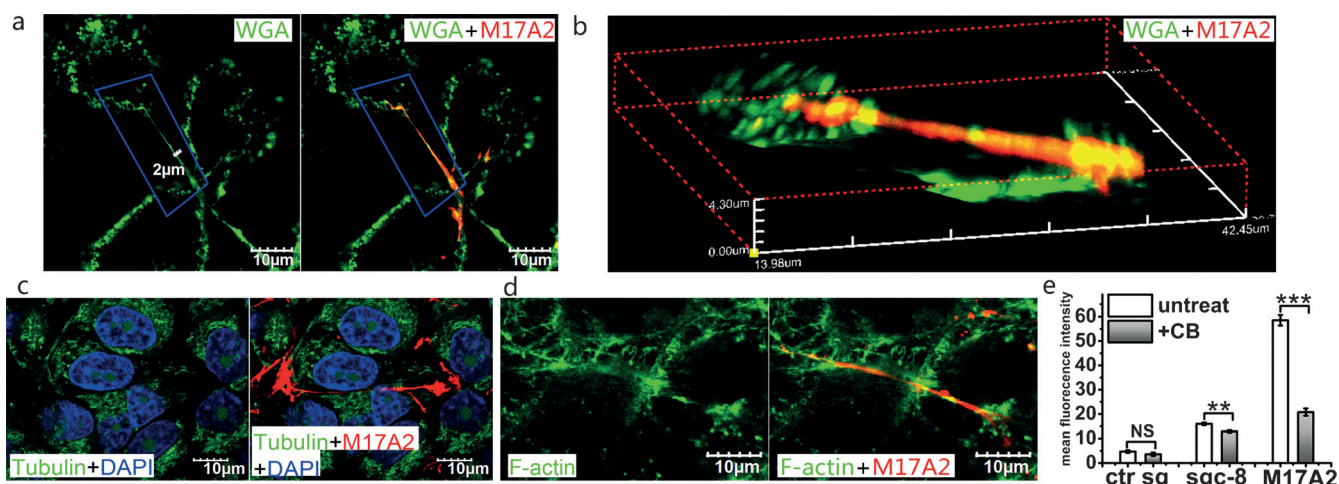


**Figure 3.** Characterization of intercellular connections recognized by M17A2. a) Confocal images of MCF-7R cells stained by FITC-WGA (green) and M17A2 (red); the scale of 2  $\mu\text{m}$  measures the diameter of the ultrafine structure. b) Z-stack image of the framed area in (a). c) MCF-7R stained by tubulin probe (green), M17A2 (red) and nuclear probe (DAPI, blue). d) MCF-7R cells stained by F-actin probe (green) and M17A2 (red). e) The binding of M17A2, sgc8, and ctr sq to MCF-7R cells treated or untreated by CB. Data are represented as mean  $\pm$  S.E. Error bars = SEM; \* $p < 0.05$ ; \*\* $p < 0.01$ ; \*\*\* $p < 0.001$ ; unpaired t-tests.

exchange of both cell-surface molecules and cytoplasmic content, including organelles, cargo vesicles, and viruses.<sup>[6,17]</sup> To demonstrate whether M17A2-binding structures were structurally linked to cell-cell crosstalk, a model of cell communication between M17A2-binding and M17A2-non-binding cells was built. MCF-7R cells were stained with vital cell tracker DiI (red) and, respectively co-cultured with MCF-7 or A549T cells (M17A2-non-binding cells) stained with vital cell tracker CFDA-SE (CFSE, blue). After culturing for at least 24 h, the cocultured cells were incubated with Cy5-labeled M17A2 (green). Confocal images showed that MCF-7 and A549T cells could not be stained by aptamer M17A2 in the absence of MCF-7R cells. However, in the co-culture system, many fluorescent regions stained by aptamer could be observed between MCF-7R cells (red), MCF-7R and MCF-7/A549T (blue) cells, and even between MCF-7 or A549T cells (Figure 4). Flow cytometry showed that M17A2 binding on MCF-7R cells slightly decreased, and it increased on M17A2-non-binding cells after co-culture, while sgc8 binding on M17A2-non-binding cells did not change after co-culture (Figure S13). These results suggest that the intercellular connections recognized by M17A2 could be built from MCF-7R cells to negative cells, and the molecular target of M17A2 was transported from MCF-7R cells to negative cells through these connecting structures.

Multidrug resistance protein 1 (MRP1) and P-glycoprotein (P-gp), common molecular pumps in the cell membrane, usually overexpress in multidrug-resistant cancer cells. As such, they are extensively studied as transporters in the context of drug resistance.<sup>[18]</sup> There is increasing evidence suggesting that P-gp could be transported from P-gp-positive cells to neighboring cells through TNTs, irrespective of cellular homology. This would result in P-gp-negative cells acquiring multidrug resistance from a “nongenetic” source.<sup>[19]</sup> Since M17A2 was generated by cell-SELEX using drug-resistant MCF-7R cells, we further investigated whether

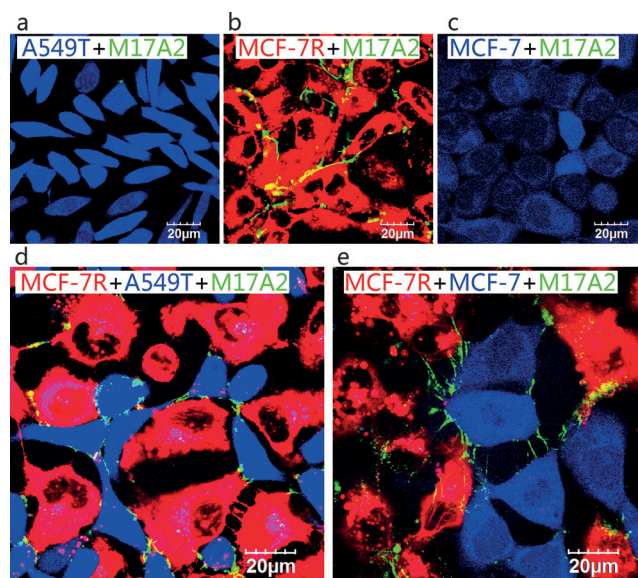


**Figure 4.** M17A2 (green) binding on different co-cultured cell lines. a) A549T; b) MCF-7R; c) MCF-7; d) co-cultured MCF-7R and A549T; e) co-cultured MCF-7R and MCF-7. A549T and MCF-7 cells were prestained by CFSE (blue). MCF-7R cells were prestained by DiI (red).

MRP1 and P-gp could be transported between cells through aptamer-binding intercellular connections. Flow cytometry analysis showed that MRP1 antibody (MRPm5) and P-gp antibody (UIC2) could bind to MCF-7R cells, but that no notable competition occurred between M17A2 and either antibody (Figure S14). Furthermore, some drug-resistant cell lines that could not bind M17A2 were found to bind either of the two antibodies (Figure S2 and S15). Confocal images with low cell density showed both antibodies binding on the cell surface, but only a very few fluorescent dots from M17A2 were observed on the cell surface (Figure 5a; Supporting

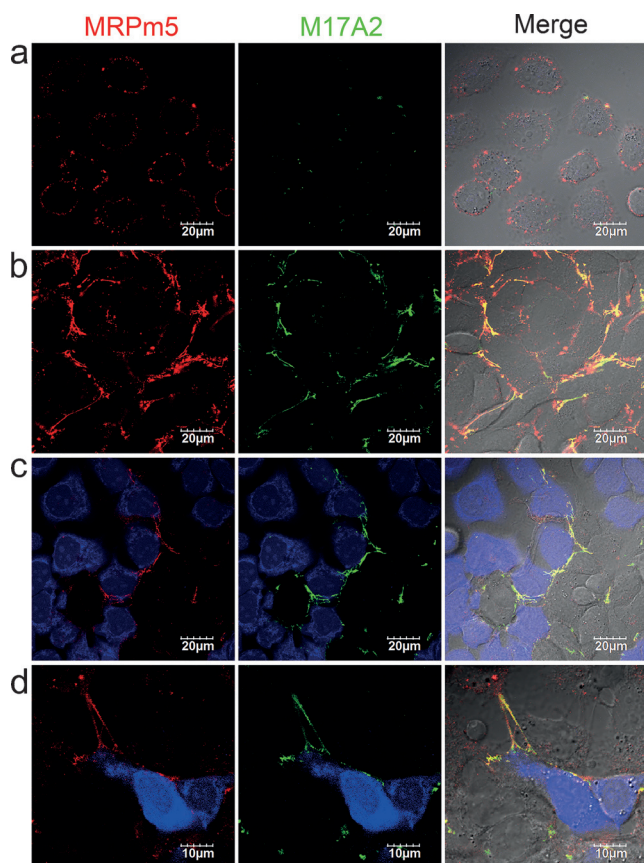


**Figure 5.** Binding of M17A2 (green) and MRP1 antibody MRPm5 (red) on different cells. a) MCF-7R cells at low density; b) MCF-7R cells at high density. c) Co-cultured MCF-7R and MCF-7 cells (blue). d) Cocultured MCF-7R and A549T cells (blue). A549T and MCF-7 cells were prestained by CFSE (blue).

Information, Figure S16b). At high cell density, antibodies bound on the surface of the cells, as well as the intercellular connections, while M17A2 mainly bound to the intercellular connections (Figure 5b; Supporting Information, Figures S16a and S17). Even on the intercellular connections, the aptamer-binding area partly overlapped with the antibody-binding area (Figure S17). These results suggest that neither MRP1 nor P-gp is the molecular target of M17A2.

Confocal images of the co-culture experiments of MCF-7 or A549T with MCF-7R showed that MRP1 was transported from MRP1-positive cells (MCF-7R) to MRP1-negative cells (MCF-7 and A549T) by routes established through intercellular connections stained by aptamer M17A2 (Figure 5c,d; Supporting Information, Figure S18). Flow cytometry also showed the decrease of the binding of MRP1 antibody and aptamer on MCF-7R cells, and the increase of them on MCF-7 cells after co-culture (Figure S19). P-gp was also observed to be transported from positive cells (MCF-7R) to negative cells (MCF-7 and A549T; Figures S20 and S21). These observations suggest that drug-resistance-related proteins could be transported to negative cells through the intercellular connections recognized by aptamer M17A2.

Unlike other aptamers and antibodies of MRP1 and P-gp that mainly bound on the surface of living cells, our results

showed that aptamer M17A2 mainly bound structures connecting cells. Among them, the long filamentous connections were identified to be TNTs. Although the morphology of other intercellular connections bound by M17A2 (much shorter and thicker than TNT) did not meet the morphological criteria of TNT, they exhibited the same cytoskeletal component and functions with TNT. It has been reported that the TNT lengths can be dynamically regulated as the connected cells migrate and the distances between them change, and TNTs break when the intercellular gap becomes too large.<sup>[8b,20]</sup> Therefore, it is reasonable to believe that the non-TNT connections bound by M17A2 have the same formation mechanism and functions with TNTs, and TNTs may be the stretched form of such connections. M17A2 was also observed to bind a few punctate regions on the body surface of cells, even isolated cells (Figure 2e; Supporting Information, Figures S9b and S11a). These punctate regions could be the precursors of these intercellular connections, which will provide clues for the investigation of the formation mechanism and growth process of these connections. We have also shown that M17A2-binding structures could be established between different cell types and could transport specific cellular proteins from positive cells to negative cells, which suggests that these connections may act as an intercellular communication route.

TNTs have been observed in many cell lines,<sup>[6]</sup> however their structures and functions are still quite unknown. Based on the morphological features and cytoskeletal component, TNT-like structures were also observed to be formed by MCF-7 cells (negative cells). However, these structures between MCF-7 cells were not bound by M17A2 or antibodies against MRP1 or P-gp, suggesting a different composition and function of TNTs formed by different cell lines. As mentioned above, TNT may be only a particular morphology of certain intercellular connections. The morphological feature is too simple to reveal the molecular signatures and function of different intercellular connections. The high selectivity of M17A2 binding to the intercellular connections between MCF-7R cells suggests that M17A2 could act as a probe to detect particular molecular signatures of such kind of intercellular connections and investigate the complex mechanism of cell–cell crosstalk, as hypothesized in this work. Further research to elucidate the identity of the molecular target of M17A2 will provide even more information about the molecular mechanism underlying the formation and functions of these intercellular connections.

In summary, we have successfully generated an aptamer, M17A2, by the cell-SELEX technique using the drug-resistant cell line MCF-7R as target cells and its parent cell line MCF-7 as negative cells. Differing from any previously reported aptamers, this aptamer specifically binds intercellular connections related to cell–cell crosstalk. More specifically, these particular intercellular connections were composed of F-actin, and some of them were further identified as TNTs or TNT-like structures based on their morphological features. When we co-cultured MCF-7R cells with other cell lines that could not form the M17A2-binding structures by monoculture, these M17A2-binding structures could be established, not only between MCF-7R cells but also between



heterologous cells, and the protein target of M17A2 could be transported from MCF-7R cells to other cell types. Multidrug resistance proteins were also found to be transported from drug-resistant MCF-7R cells to drug-sensitive MCF-7 cells through these intercellular connections. In light of these findings, aptamer M17A2 could act as a new probe to investigate cell–cell communication through intercellular connections.

## Acknowledgements

We gratefully acknowledge financial support from the 973 Program (grants 2011CB911000 and 2013CB933700) and NSF of China (grants 21275149, 21375135, 21575147, 21535009, and 21321003).

**Keywords:** aptamers · cell communication · fluorescent probes · intercellular connections · tunneling nanotubes

**How to cite:** *Angew. Chem. Int. Ed.* **2016**, 55, 3914–3918  
*Angew. Chem.* **2016**, 128, 3982–3986

- [1] J. Pasquier, B. S. Guerrouahen, H. Al Thawadi, P. Ghiabi, M. Maleki, N. Abu-Kaoud, A. Jacob, M. Mirshahi, L. Galas, S. Rafii, F. Le Foll, A. Rafii, *J. Transl. Med.* **2013**, 11, 94.
- [2] C. Thery, L. Zitvogel, S. Amigorena, *Nat. Rev. Immunol.* **2002**, 2, 569–579.
- [3] A. Ito-Ishida, S. Okabe, M. Yuzaki, *Neurosci. Res.* **2014**, 83, 64–68.
- [4] N. Defamie, A. Chepied, M. Mesnil, *FEBS Lett.* **2014**, 588, 1331–1338.
- [5] J. Faix, D. Breitsprecher, T. E. Stradal, K. Rottner, *Int. J. Biochem. Cell Biol.* **2009**, 41, 1656–1664.
- [6] a) F. A. Ramírez-Weber, T. B. Kornberg, *Cell* **1999**, 97, 599–607; b) B. Onfelt, S. Nedvetzki, K. Yanagi, D. M. Davis, *J. Immunol.* **2004**, 173, 1511–1513; c) A. Rustom, R. Saffrich, I. Markovic, P. Walther, H. H. Gerdes, *Science* **2004**, 303, 1007–1010; d) E. Y. Plotnikov, T. G. Khryapenkova, A. K. Vasileva, M. V. Marey, S. I. Galkina, N. K. Isaev, E. V. Sheval, V. Y. Polyakov, G. T. Sukhikh, D. B. Zorov, *J. Cell. Mol. Med.* **2008**, 12, 1622–1631; e) A. Chauveau, A. Aucher, P. Eissmann, E. Vivier, D. M. Davis, *Proc. Natl. Acad. Sci. USA* **2010**, 107, 5545–5550; f) X. Wang, M. L. Veruki, N. V. Bukoreshtliev, E. Hartveit, H. H. Gerdes, *Proc. Natl. Acad. Sci. USA* **2010**, 107, 17194–17199; g) K. M. He, X. L. Shi, X. J. Zhang, S. Dang, X. W. Ma, F. Liu, M. Xu, Z. Z. Lv, D. Han, X. H. Fang, Y. Y. Zhang, *Cardiovasc. Res.* **2011**, 92, 39–47.
- [7] D. M. Davis, S. Sowinski, *Nat. Rev. Mol. Cell Biol.* **2008**, 9, 431–436.
- [8] a) H. H. Gerdes, R. N. Carvalho, *Curr. Opin. Cell Biol.* **2008**, 20, 470–475; b) M. W. Austefjord, H. H. Gerdes, X. Wang, *Commun. Integr. Biol.* **2014**, 7, e27934.
- [9] a) A. D. Ellington, J. W. Szostak, *Nature* **1990**, 346, 818–822; b) C. Tuerk, L. Gold, *Science* **1990**, 249, 505–510.
- [10] a) D. Shangguan, Y. Li, Z. W. Tang, Z. H. C. Cao, H. W. Chen, P. Mallikaratchy, K. Sefah, C. Y. J. Yang, W. H. Tan, *Proc. Natl. Acad. Sci. USA* **2006**, 103, 11838–11843; b) K. Sefah, D. Shangguan, X. L. Xiong, M. B. O'Donoghue, W. H. Tan, *Nat. Protoc.* **2010**, 5, 1169–1185.
- [11] M. S. L. Raddatz, A. Dolf, E. Endl, P. Knolle, M. Famulok, G. Mayer, *Angew. Chem. Int. Ed.* **2008**, 47, 5190–5193; *Angew. Chem.* **2008**, 120, 5268–5271.
- [12] a) T. Bing, X. J. Liu, X. H. Cheng, Z. H. Cao, D. H. Shangguan, *Biosens. Bioelectron.* **2010**, 25, 1487–1492; b) G. Mayer, M. S. L. Ahmed, A. Dolf, E. Endl, P. A. Knolle, M. Famulok, *Nat. Protoc.* **2010**, 5, 1993–2004; c) H. C. Mei, T. Bing, X. J. Yang, C. Qi, T. J. Chang, X. J. Liu, Z. H. Cao, D. H. Shangguan, *Anal. Chem.* **2012**, 84, 7323–7329; d) J. L. Vinkenborg, G. Mayer, M. Famulok, *Angew. Chem. Int. Ed.* **2012**, 51, 9176–9180; *Angew. Chem.* **2012**, 124, 9311–9315; e) C. Qi, T. Bing, H. C. Mei, X. J. Yang, X. J. Liu, D. H. Shangguan, *Biosens. Bioelectron.* **2013**, 41, 157–162; f) W. Tan, M. J. Donovan, J. Jiang, *Chem. Rev.* **2013**, 113, 2842–2862.
- [13] J. N. Zadeh, C. D. Steenberg, J. S. Bois, B. R. Wolfe, M. B. Pierce, A. R. Khan, R. M. Dirks, N. A. Pierce, *J. Comput. Chem.* **2011**, 32, 170–173.
- [14] D. Shangguan, Z. H. Cao, L. Meng, P. Mallikaratchy, K. Sefah, H. Wang, Y. Li, W. H. Tan, *J. Proteome Res.* **2008**, 7, 2133–2139.
- [15] N. M. Sherer, W. Mothes, *Trends Cell Biol.* **2008**, 18, 414–420.
- [16] N. V. Bukoreshtliev, X. Wang, E. Hodneland, S. Gurke, J. F. Barroso, H. H. Gerdes, *FEBS Lett.* **2009**, 583, 1481–1488.
- [17] a) K. Gousset, E. Schiff, C. Langevin, Z. Marijanovic, A. Caputo, D. T. Browman, N. Chenouard, F. de Chaumont, A. Martino, J. Enninga, J. C. Olivo-Marin, D. Mannel, C. Zurzolo, *Nat. Cell Biol.* **2009**, 11, 328–336; b) E. A. Eugenin, P. J. Gaskill, J. W. Berman, *Cell. Immunol.* **2009**, 254, 142–148.
- [18] a) A. Levchenko, B. M. Mehta, X. L. Niu, G. Kang, L. Villafania, D. Way, D. Polycarpe, M. Sadeain, S. M. Larson, *Proc. Natl. Acad. Sci. USA* **2005**, 102, 1933–1938; b) O. Kovalchuk, J. Filkowski, J. Meservy, Y. Ilnytskyy, V. P. Tryndyak, V. F. Chekhun, I. P. Pogribny, *Mol. Cancer Ther.* **2008**, 7, 2152–2159.
- [19] J. Pasquier, L. Galas, C. Boulange-Lecomte, D. Rioult, F. Bultelle, P. Magal, G. Webb, F. Le Foll, *J. Biol. Chem.* **2012**, 287, 7374–7387.
- [20] S. Sowinski, C. Jolly, O. Berninghausen, M. A. Purbhoo, A. Chauveau, K. Kohler, S. Oddos, P. Eissmann, F. M. Brodsky, C. Hopkins, B. Onfelt, Q. Sattentau, D. M. Davis, *Nat. Cell Biol.* **2008**, 10, 211–219.

Received: November 20, 2015

Revised: January 26, 2016

Published online: February 17, 2016